Polymer 50 (2009) 1005–1014

Contents lists available at ScienceDirect

Polymer

journal homepage: www.elsevier.com/locate/polymer

Synthesis, characterization and swelling behaviour of poly(methacrylic acid) brushes synthesized using atom transfer radical polymerization

Andrew J. Parnell [a,*], Simon J. Martin [b], Cheen C. Dang [a], Mark Geoghegan [a], Richard A.L. Jones [a], Colin J. Crook [c], Jonathan R. Howse [d], Anthony J. Ryan [c]

[a] Department of Physics and Astronomy, The University of Sheffield, The Hicks Building, Sheffield S3 7RH, UK
[b] IPTME, Loughborough University, Loughborough LE11 3TU, UK
[c] Department of Chemistry, The University of Sheffield, Sheffield S3 7HF, UK
[d] Department of Chemical and Process Engineering, The University of Sheffield, Sheffield S1 3JD, UK

ARTICLE INFO

Article history:
Received 26 August 2008
Received in revised form
26 November 2008
Accepted 27 November 2008
Available online 9 December 2008

Keywords:
AFM
Brush
Polyelectrolyte

ABSTRACT

Poly(methacrylic acid) brushes have been prepared utilizing the "grafting from" technique and a living radical synthesis route using a two stage process. Firstly a poly(1-ethoxyethyl methacrylate) brush was synthesized by atom transfer radical polymerization and then thermally decomposed to poly(methacrylic acid). The swelling behaviour of the weak polyacid brush was investigated as a function of pH and salt concentration in aqueous solutions using atomic force microscopy. Force pulling measurements were used to establish the molecular weight and the grafted chain density. The swelling transition was found to be at pH 9; which is significantly different to the pK_a (5.5) of untethered poly(methacrylic acid). We attribute this large shift in pK_a to the high grafting density of these brushes. This can be explained as a result of the Coulombic repulsion of neighbouring charges. High salt concentrations (0.3 M Na^+) also collapse the brush layer. Conversely low salt concentrations cause an increase in the thickness of the brush, a behaviour expected for osmotic brushes.

1. Introduction

A polymer brush is a collection of polymer chains that are grafted to a surface or interface at sufficiently high densities that the polymer chains are forced to adopt a stretched conformation away from the surface to reduce segment–segment interactions. Polymer brushes offer a route for tuning surface properties by choosing a suitable functionality for a specified application. Brush layers can be synthesized that are responsive to an environmental stimulus; generating so called "smart" polymer systems. Surfaces that respond to a vast array of stimuli such as solvent quality, temperature, light and electrical potentials are very desirable. The possible applications for these smart surfaces include: directing cellular function, drug delivery, lubrication, and the detection of biomolecules. Valves and openings can be coated with polyelectrolytes to allow molecular sorting with the potential to retain proteins and release proteins on demand [1]; responsive brushes have the possibility to be used as a new class of nano-actuating materials [2,3].

Polyelectrolyte brushes are capable of switching conformation in response to changes in pH, ionic strength or the valency of the salt enabling the tailoring of the surface properties [4]. The degree of swelling and the range of pH values over which the layer switches conformation can be tailored by altering the grafting density and chain architecture [5].

Polymer brushes are usually formed by grafting the polymer onto a surface or interface. One end of the polymer is functionalized so that it can react with an appropriate surface, typically using thiol or silane chemistry although physisorption with a diblock copolymer can also be used [6,7]. The advantage of the "grafting to" method is that there is precise control over the molecular weight and the polydispersity of the polymer system on the surface, as modern synthesis routes like anionic polymerization can give excellent control over these properties. Entropic effects limit the grafting density of brushes formed in this fashion, as the chains will spread out in order to maximize their conformational entropy, which reduces the area available for other chains to reach the surface.

Another way to prepare brushes is to grow the polymers in situ from an initiator on the surface, the so-called "grafting from" method. This method allows the growth of high density brushes as

* Corresponding author. Tel.: +44 (0)114 222 3505.
E-mail address: a.j.parnell@sheffield.ac.uk (A.J. Parnell).

0032-3861/$ – see front matter © 2008 Elsevier Ltd. All rights reserved.
doi:10.1016/j.polymer.2008.11.051

the entropic effects that limit the densities of brushes produced via "grafting to" route do not apply. The "grafting from" method used in this work involves depositing a monolayer of an initiating species onto a surface or interface from which a polymer chain can then be "grown" using atom transfer radical polymerization (ATRP). This can be a living polymerization mechanism and so gives control over the molecular weight and polydispersity of the polymer brush. Determining the exact molecular weight can be problematic however, due to the inability to measure the molecular weight directly from the grafted brush layer using standard GPC techniques. As an area of 1 cm^2 contains approximately 2.5 μg of material for a 25 nm thick brush layer of PMAA, assuming successful cleavage from the silicon substrate which is non-trivial with our present system. Polymer bulk laboratory methods for determining molecular weight (i.e. size exclusion chromatography) require milligrams of material and can therefore not be used. Free initiator can also be added to the polymerization reaction to determine the molecular weight of the brush indirectly [8].

The primary condition for the onset of brush like behaviour is that the distance between polymer chain grafting sites be significantly less than radius of gyration (R_g) of the polymer [9]. Here the height of the brush scales linearly with the polymerization index N, whereas an unstretched chain would scale as $N^{1/2}$ [10]. Brushes are stretched and it is this stretching that makes them different and therefore interesting compared to ungrafted chains in solution. Other types of deposited polymer layer architectures such as spin coated layers and layer by layer deposited systems are less confined and will consequently adopt a random walk configuration in solution. For these systems the actuation comes from the globule to coil transition and most systems tend to be hydrogel layers and form a network of linked chains [11].

The properties of grafted weak polyelectrolytes in solution are significantly more complex than those of grafted strong polyelectrolytes as the charge density is not fixed for weak polyelectrolytes [12]. Instead the charge density varies depending on the pH or ionic strength of the surrounding solution [13–16]. Weak polyelectrolytes exhibit much richer behaviour in response to added salt ions than either strong polyelectrolytes or neutral brushes. Weak polyelectrolyte brushes collapse in the same way as strong polyelectrolyte brushes at high salt concentrations. However weak polyelectrolyte brushes exhibit an interesting effect before this critical collapse salt concentration is reached; at low (increasing) salt concentrations the brush height increases and this is referred to as the osmotic brush state. This happens due to the requirement of charge neutrality for the local concentration of protons in the brush. As the salt ions can be exchanged with the protons without invalidating the charge neutrality requirement, the salt ions have the effect of altering the degree of dissociation of the acid or base groups depending on whether the brush is a polyacid or a polybase. It is likely that the salt cations (e.g. Na^+) will recombine with the acid groups in a polyacid brush to form a salt [17]. This leads to a net increase in the charge within the system, causing an increase in the osmotic pressure within the brush. Consequently the brush swells with increasing salt concentration until the salted brush regime is reached and the brush collapses [18]. The crossover regime between the osmotic brush state and the salted brush should take place when the external salt concentration corresponds to the concentration of free ions inside the brush.

In this work we report the synthesis and characterization of poly(methacrylic acid) (PMAA) brushes using a protected monomer that can be deprotected to give well-defined PMAA brushes. PMAA is an example of a weak polyacid that exhibits a large volumetric change when it passes through its collapse transition making it an ideal model system for study. ATRP gives control over molecular weight and polydispersity and is available for a wide range of monomers, but unfortunately PMAA is difficult to synthesize directly via ATRP because the acidic monomers poison the catalyst by coordinating to the transition metal [19]. To overcome this problem a two-step process is utilised. A brush of poly(1-ethoxyethyl methacrylate) is grown via ATRP and then thermally converted to PMAA.

The response of the brushes to the addition of salt and the variation of the solution pH was investigated using atomic force microscopy (AFM) in liquid. This is a technique that has been used by many researchers looking at brush response and dynamics [20,21]. We show that the swelling transition occurs at significantly higher pH values than that observed for the free untethered polymer [22]. The molecular weight of the grafted brush was determined with high resolution force spectroscopy (HRFS), by force pulling measurements of the chains pulled out of the brush and measuring the terminal distance and equating this to be the molecular weight of the brush.

2. Experiment

2.1. Substrate preparation

Silicon wafers (Mitsubishi Research) polished to the (100) face and having a native oxide layer thickness of 15 Å, and rendered hydrophilic by first cleaning in an oxygen plasma for 10 min followed by the RCA method stage one [23] (18 MΩ cm water, ammonia (BDH 37%) and hydrogen peroxide (Fisher) (20% v/v) with a volume ratio of 5:1:1, at 80 °C for 10 min). The sample was then washed repeatedly with clean water. The cleaned silicon was dried under a nitrogen atmosphere for several minutes and placed in a vacuum oven at 80 °C for 30 min to remove all the traces of water on the silicon surface. The initiator (11-(2-bromo-2-methyl)-propionyloxy)undecyl trichlorosilane was synthesized according to the method used by Beers et al. [24,25]. Copper(I) chloride (Aldrich, 98%+) was purified using sequential washings with glacial acetic acid under nitrogen, petroleum ether and ethanol before storing under nitrogen. Triethylamine (Aldrich, 99%) was filtered through a 0.45 μm PTFE Acrodisc CR filter (PALL Life Sciences) immediately prior to use. *N*,*N*,*N*′,*N*′,*N*″-pentamethyldiethylenetriamine (PMDETA, Aldrich, 99%) and methyl-2-bromopropionate (Aldrich, 98%) were used as-received. The silicon surface was rendered hydrophilic as described above before being sealed tightly in a PTFE beaker containing 20 mL of a 0.15% v/v solution of (11-(2-bromo-2-methyl)propionyloxy)undecyl trichlorosilane initiator in dry toluene [26]. The silicon block was then removed and subjected to two sequential washings with toluene, acetone, and ethanol before finally being dried under nitrogen. The blocks were stored under vacuum until required for the brush synthesis. Decyltrichlorosilane (Aldrich) was used as the non-initiating species for the variable grafting density study also at a concentration of 0.15% v/v in dry toluene.

2.2. Synthesis of 1-ethoxyethyl methacrylate (EEMA)

Under a nitrogen atmosphere, 1.0 mol (85.2 mL) of methacrylic acid (Aldrich 99%) was added slowly at 0 °C to a mixture of 1.2 mol (114.9 mL) of ethyl vinyl ether (Aldrich 99%) and 0.002 mol (0.2 g) of phosphoric acid (Aldrich) as a catalyst. The mixture was stirred at room temperature for 48 h. The catalyst was then absorbed in hydrogen talcite. After filtration the excess vinyl ether was evaporated using a rotary evaporator. The product was distilled at reduced pressure to remove the phenothiazine polymerization inhibitor. The product was stored at −10 °C prior to use [27,28]. The ^{1}H NMR (chloroform-d) for the EEMA monomer is displayed in Fig. 1 and confirms the structure of the EEMA monomer.

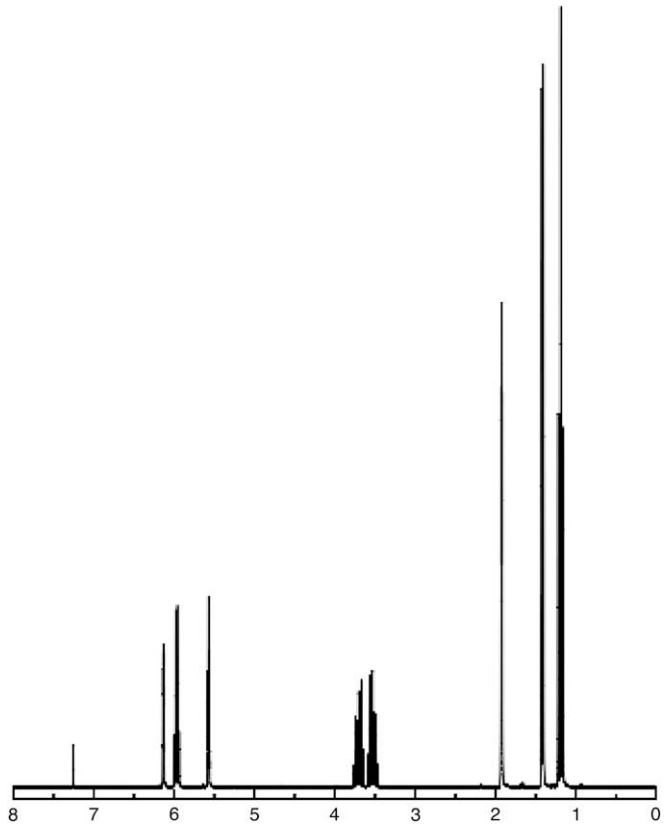

Fig. 1. ^{1}H NMR data for the EEMA monomer prior to the synthesis. 1.21 [3H, t, –OCH$_2$C*H*$_3$], 1.43 [3H, d, –COOCH(C*H*$_3$)], 1.95 [3H, s, CH$_2$=C(C*H*$_3$)], 3.52–3.75 [2H, m, –OC*H*$_2$–], 5.59 [1H, s, C*H*$_2$=C(CH$_3$)–], 5.99 [1H, q, –COOC*H*(CH$_3$)], 6.15 [1H, s, C*H*$_2$=C(CH$_3$)–].

2.3. ATRP procedure for 1-ethoxyethyl methacrylate synthesis

The EEMA monomer was passed through a column of basic Al_2O_3 (BDH) to remove any unreacted methacrylic acid or other impurities. The EEMA monomer (21 mL) was then placed into the reaction vessel. The Cu(I)Cl (75 mg) was weighed out and placed into the reaction vessel and stirred continuously until the wafers were removed. The reaction vessel was purged for 15 min with oxygen free nitrogen (BOC) after which time 0.6 mL of the ligand (PMDETA) was added through a suba-seal using a syringe. After the addition of the ligand the silicon wafers were lowered into the ATRP mixture and the polymerization proceeded for a maximum of 2 h depending on the desired brush thickness. The polymerization was carried out at room temperature.

2.4. Procedure for the deprotection of 1-ethoxyethyl methacrylate to methacrylic acid

It is possible to synthesize PMAA brushes with poly(*tert* butyl acrylate) [12,29,30] as the precursor which can then be hydrolysed under strong acidic conditions to leave a brush layer that is inhomogeneous over the surface. We prefer to use an EEMA synthesis because the conversion to PMAA is achieved without the use of harsh reaction conditions that could cause cleavage of the brush chains Scheme 1. The hydrolysis is performed by heating the brush to 150 °C in a vacuum oven for 4 h (hydrolysis step 1) and then placing it in water (hydrolysis step 2). The effect of the heating is to remove the protecting groups and leave a poly(methacrylic acid) brush; further heating could result in anhydride formation. This was overcome by placing each brush in ultrapure deionized water for a minimum of 24 h. The anhydride group is highly reactive and is readily converted back to a carboxylic acid group via this method.

2.5. Characterization

The thickness of the polymer brushes was measured using ellipsometry. A Gaertner 116B ellipsometer using a HeNe laser at 628 nm and 70° incidence angle was used. The resulting ellipsometric parameters Ψ and Δ were fitted using a single layer model with a refractive index of $n = 1.5$ on a silicon substrate with values for the real (n) and imaginary components (k) of $n = 3.875$ and $k = 0.018$. Ten measurements were taken over the sample surface and the data presented here are the average values obtained with the associated standard deviation.

The chemical composition of the brush was investigated using a Perkin Elmer Spectrum One FTIR spectrometer. The samples for

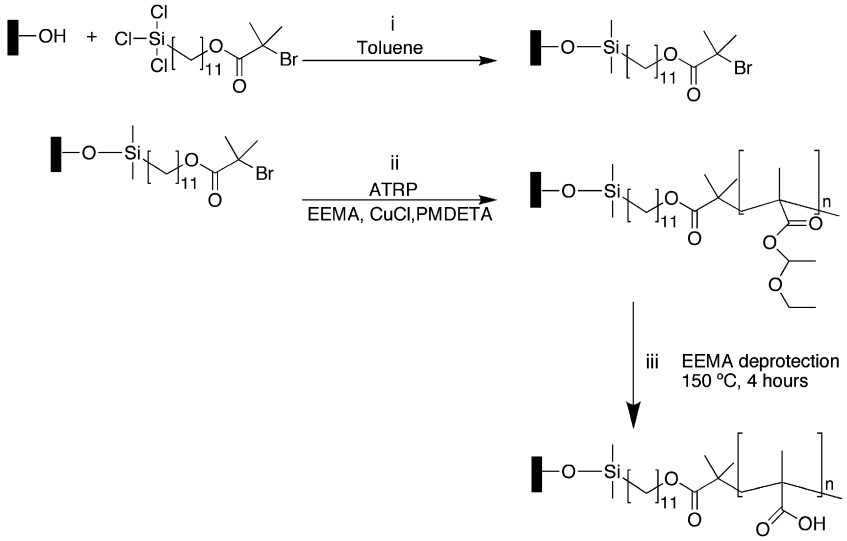

Scheme 1. The reaction scheme for the growth of a protected poly(1-ethoxyethyl methacrylate) brushes on silicon substrates, (step i) is attachment of the initiator to the silicon surface. Followed by the brush polymerization (step ii) and subsequent conversion to poly(methacrylic acid) via a pyrolysis de-protection stage (step iii).

this study were grown on both sides of ultra thin silicon wafers (50 μm thick) polished on both sides (Virginia Semiconductor).

The sessile or "static" drop method was used to determine the advancing contact angles, with water as the liquid phase. An FTA 200 machine (First Ten Angstroms) was used in conjunction with the inbuilt drop shape analysis software to determine the plateau point in the drop formation, corresponding to the advancing contact angle for the surface being measured. For each surface three areas were measured to give an average contact angle. Between each measurement, the samples were rinsed in ultrapure water (resistivity of 18 MΩ cm) and dried under nitrogen. The brush samples used in the study were measured before and after the hydrolysis to see its effect on the contact angle. To study the effect of the pH, the solution was adjusted using concentrated HCl (BDH) or NaOH (BDH).

The X-ray photoelectron spectroscopy (XPS) wide energy scan data are plotted in Fig. 2; a scan is performed at each step in the scheme for synthesizing a PMAA brush layer. Each sample studied was measured at three separate areas on the brush surface to examine the homogeneity of the ATRP reaction scheme. The samples were studied at a take-off angle of 90°. The data were subsequently analysed using the standard CASA (XPS) software package. The RCA cleaned silicon and initiator-treated silicon stages have spectra dominated by the underlying silicon surface. The XPS data shown in the inset in Fig. 2 confirm the successful formation of the initiator layer with a bromine 3d peak at 69.7 eV.

2.5.1. Instrumentation

A Nanoscope IIIA multi-mode AFM manufactured by Veeco (Santa Barbara) was used for the ambient air condition scans of the brush layers. The AFM tips were standard Olympus tapping tips with a resonance of 275 kHz. A Dimension 3100 AFM was used with a Nanoscope IV controller for the liquid measurements. This configuration of the Dimension AFM provides the most suitable setup for altering the pH because the sample can be accessed with ease, due to the open configuration of the sample and scan head. A section of the brush layer was removed using a scalpel to leave a brush silicon-boundary that was then imaged as the pH or ionic strength was altered. The pH of the solution was measured immediately prior to each pH change and then added using a micropipette. The pH of each solution was measured with a Seven Easy pH meter (Mettler Toledo) calibrated using buffer solutions of pH 3, pH 7 and pH 9.2 (Scientific Laboratory Supplies). Initially the sample was overfilled with an excess of the new pH solution, which was then removed with a clean micropipette. This process was repeated 4–5 times to make sure that the pH of the solution was well defined. The same procedure was carried out for the added salt experiments. The salt sodium nitrate ($NaNO_3$, 99%) (Aldrich) was chosen as it contains only monovalent ions, the pH of the solution that of deionized water (pH 6.5). Brush samples were then imaged for 25 min per pH environment or ionic strength as this allowed the sample to equilibrate, with the last image being used for the brush height measurement. An experimental study of the brush response dynamics has shown this to be sufficient for the brush layer to swell, with a typical layer responding to the influence of the solvent pH in seconds to tens of seconds [22]. The analysis of the AFM images involved measuring the step height change in the brush as a function of the solution pH. This was done across the same scan region to remove uncertainties due to fluctuations in sample thickness. The brush height was determined from an average of 6 line scans to give a brush layer thickness for each particular pH or ionic strength.

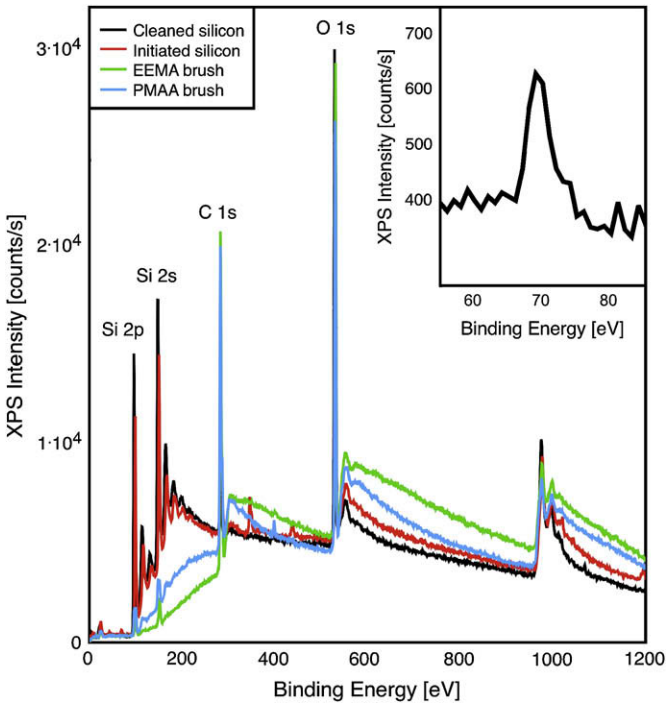

Fig. 2. XPS data from the surface of the brush layers, these data were used to determine the atomic composition of the brush layers and to infer the conversion of the brushes from protected PEEMA to PMAA. The inset figure is of the bromine 3d peak at 69.7 eV for the initiator coated silicon.

High resolution force measurements were made using a Molecular Force Probe 1D instrument (MFP, Asylum Research, Inc.) isolated from vibrations using a Halcyonics active vibration table. The experimental setup uses an open cell arrangement with a wetted SPM tip brought into contact with the wetted sample surface. Commercially available soft cantilevers (MSCT-AUNM Veeco SPM) were used which had ultra sharp, gold-coated (increased reflectivity) silicon nitride tips calibrated using the thermal method built into the MFP. The tips had a radius of curvature of less than 20 nm. The spring constant for each experiment was determined according to the nondestructive thermal method [31].

The brush samples were cleaned with copious amounts of deionized water before and after each set of measurements and allowed to equilibrate with the solution for 5–10 min. This timescale proved more than adequate as no noticeable change in the force curve data was observed over this timescale. The pulling speed of the cantilever tip was kept constant for all data at 800 nm s^{-1} and the tip reversed and approached with no dwell time on the surface. The Asylum MFP 1D was used for all the force pulling measurements with the force separation data converted into force–distance data using the methodology of Seog et al. [32]. The MFP measures force as a function of the cantilever deflection along the z-axis. This observed deflection is made up of the distance between the tip and the sample and the cantilever deflection, so for a true value of the tip-sample distance D and to produce meaningful force–distance curves, the cantilever deflection must be subtracted from the z-piezo movement to give values for D. For a very hard surface, zero separation is defined as the region in the force curve in which the cantilever deflection is coupled 1:1 with the sample movement. This appears in the force curve as a straight line of unit slope. A complete force curve includes the measured force as the tip probe approaches the sample and is retracted to its initial starting position.

X-ray reflectivity measurements of the brush sample was made using a Bruker D8 Advance X-ray scattering system fitted with a Göbel mirror on the X-ray source emitting radiation at 1.54 Å

(copper Kα) and running at 40 kV and 40 A. The sample was a 50 mm diameter circular silicon wafer. Reflectivity runs were collected over a 4 h period with step sizes sufficiently small enough to distinguish the features seen. The data were fitted using custom written routines with the application pro Fit (QuantumSoft) for the Macintosh. The brush layer was modeled as a stack of thin slabs using a recursive scheme [33,34]. Each layer within the model was characterized by an X-ray density, a thickness and a roughness modelled following the scheme of Névot and Croce [35]. The data fitting was done in a least-squares manner. A combination of steepest descent and Monte Carlo fitting procedures was used in order to ensure that the fits obtained were as close as possible to the global minima.

3. Results

3.1. Growth of 1-ethoxyethyl methacrylate brushes and their subsequent conversion to poly(methacrylic acid)

The kinetics of the ATRP 'living' polymerization reaction used to synthesize the brushes was investigated using an eight armed reaction vessel which enabled the removal of silicon wafers at set times throughout the reaction. (The reaction vessel is kept under a positive pressure of nitrogen gas, ensuring that the reaction continues unaffected during removal of the silicon wafers.)

Fig. 3 shows ellipsometry measurements for the increase in brush thickness as a function of the reaction time for a series of brushes before and after the thickness change following deprotection/removal of the protecting group. The first 30 min of the polymerization shows a linear growth rate in the brush thickness until a thickness of 30 nm after which the reaction appears to slow with no further increase in thickness. This could be due to a number of possible factors including poisoning of the reaction by oxygen in the reaction system and also the burying of the living ends in the bulk of the brush, reducing the reaction rate [36]. Another mechanism could be a small amount of chain deprotection that would inhibit further brush growth. The difference in thickness between the hydrolyzed and unhydrolyzed brushes is a key indication of the change from PEEMA to PMAA as the bulky protecting groups have been removed from the chain. This thickness change is very pronounced with the PMAA brush layer being thinner after the deprotection step than the unhydrolysed PEEMA and gives a qualitative confirmation that the hydrolysis step has converted the protected monomer to poly(methacrylic acid). A calculation of the thickness change from the removal of the bulky protecting group during the heating step predicts a thickness reduction of 46% as the PEEMA is converted to PMAA. The sample polymerized for 90 min was initially 31.6 nm and reduced to 17.9 nm after heating. We predict (assuming the mass change under hydrolysis) the brush to have a thickness of 17.1 nm, which agrees well with the observed thickness change for the PEEMA brush.

A simple way of confirming that the pyrolysis of EEMA to poly(methacrylic acid) is effective at hydrolyzing the brush layer is to

Table 1
Contact angle data for the various stages in the preparation of EEMA brushes and subsequent conversion to PMAA brushes.

Sample	Configuration	Advancing water contact angle
RCA cleaned silicon	Si/SiO_2	12°
Initiated layer of silicon	Si/SiO_2/Init	73°
Brush A unhydrolyzed	Si/SiO_2/Init/PEEMA	76°
Brush B unhydrolyzed	Si/SiO_2/Init/PEEMA	75°
Brush A hydrolyzed	Si/SiO_2/Init/PMAA	35°
Brush B hydrolyzed	Si/SiO_2/Init/PMAA	33°

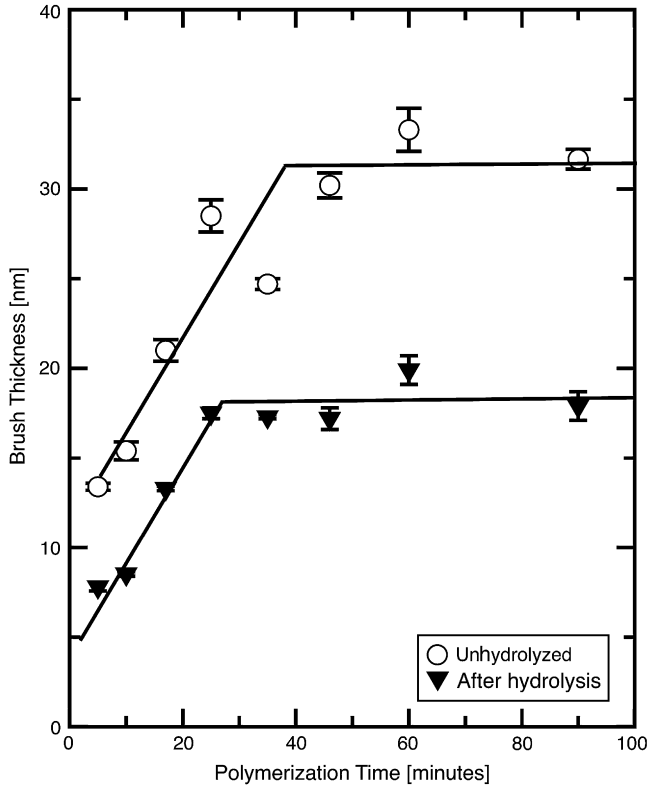

Fig. 3. Polymer brush thickness as a function of the polymerization time for the 1-ethoxyethyl methacrylate (circles) and after the hydrolysis to poly(methacrylic acid).

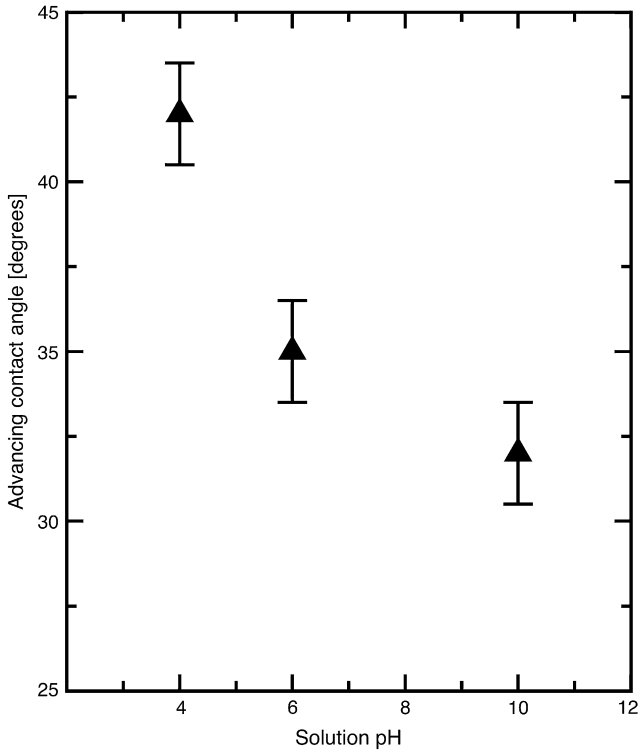

Fig. 4. Static water contact angle measurements as a function of pH for a PMAA brush.

measure the contact angle of water drops on the brush layers at the different stages of brush treatment. The contact angle value for RCA cleaned silicon of 12° compares well with the literature value [37] of 10° for the type of silicon used. Table 1 shows that the contact angle of the brush surface for two identical brushes is consistent and also that the change in contact angle after hydrolysis is very pronounced. Contact angle measurements are a means of examining changes in the surface energy but these measurements do not elucidate whether the brush is fully hydrolyzed throughout because it only probes the top 10–20 Å of the brush layer. To test the polyelectrolytic nature of the brush layer contact angles at different values of pH were measured for the collapsed (pH 4), and swollen (pH 10) states of the brush; the data are presented in Fig. 4. The data for the pH change from pH 4 to pH 10 show a shift in the contact angle from 42° for the collapsed layer down to 32° for the swollen state. The value of the contact angle for the brush at pH 10 is similar to the value at pH 6 (35°), even though we noted the swelling transition using AFM measurements to take place above pH 9. However dilute PMAA is expected to be swollen at pH 6, and our earlier measurements on polybase brushes demonstrated that the end of the brush is more likely to be swollen than the region close to the substrate [38].

FTIR is a powerful tool for examining the chemical composition of samples. Brushes must be grown on thin IR transparent silicon (silicon has a transmission window in the IR region), enabling the absorption spectrum of the brush to be measured. This was done using thin silicon polished on both sides to give sufficient transmission to measure the IR spectrum. The homopolymer data presented in Fig. 5 show the spectrum for a PMAA standard (Polymer Source) with a broad peak at 3200 cm^{-1} which is attributed to the –OH group [6]. Confirmation of the chemical conversion of the brush layer can be seen in the IR spectra in Fig. 5. The most important change in the spectrum after hydrolysis is the growth of an extremely broad peak due to the carboxylic acid O–H stretch from 3500 to 2500 cm^{-1}. We also note a broadening of the carbonyl stretch due to overlapping monomeric 1704 cm^{-1} and dimeric 1724 cm^{-1} acid bands and a reduction in the 1140 cm^{-1} peak from the C–O–C group.

The wide scan X-ray photoelectron spectroscopy data (Fig. 2) confirm the transformation of the brush to PMAA via the removal of the 1 ethoxy-ethyl protecting group by a change in the surface composition of 68:25 (C:O)–60:28 (C:O). For EEMA the molar ratio between carbon and oxygen is 8:3 so a 68% composition gives an oxygen value of 25.5% very close to the measured value of 25%. After heating if the layer had not been converted successfully this would give a ratio of 60:22.5. Whereas the molar ratio of C:O for PMAA is 4:2, again for a 60% carbon composition we would expect a 30% oxygen composition, again close to the measured value of 28%. The measured change in the carbon/oxygen ratio using XPS shows the successful deprotection and conversion of the brush layer to PMAA.

To summarize, the conversion of the protected PEEMA to PMAA has been demonstrated using FTIR, XPS, contact angle and ellipsometry measurements.

The surface Fig. 6 uniformity of the brushes has been demonstrated by using both X-ray reflectivity (Fig. 6) and AFM (see Supporting information) on similar samples. The brush layer is clearly uniform with a root mean square roughness value of 0.5 nm determined independently from both measurements.

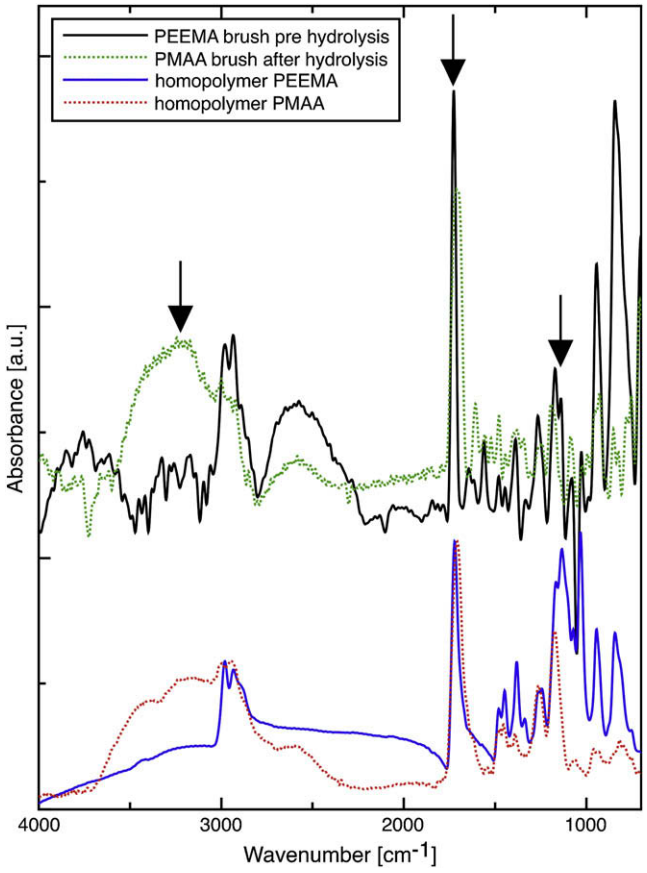

Fig. 5. FTIR spectra for a brush before and after the conversion of the grafted brush layer from poly(1-ethoxyethyl methacrylate) to poly(methacrylic acid) via a pyrolysis step. The arrows highlight the main changes after conversion to PMAA (see main text).

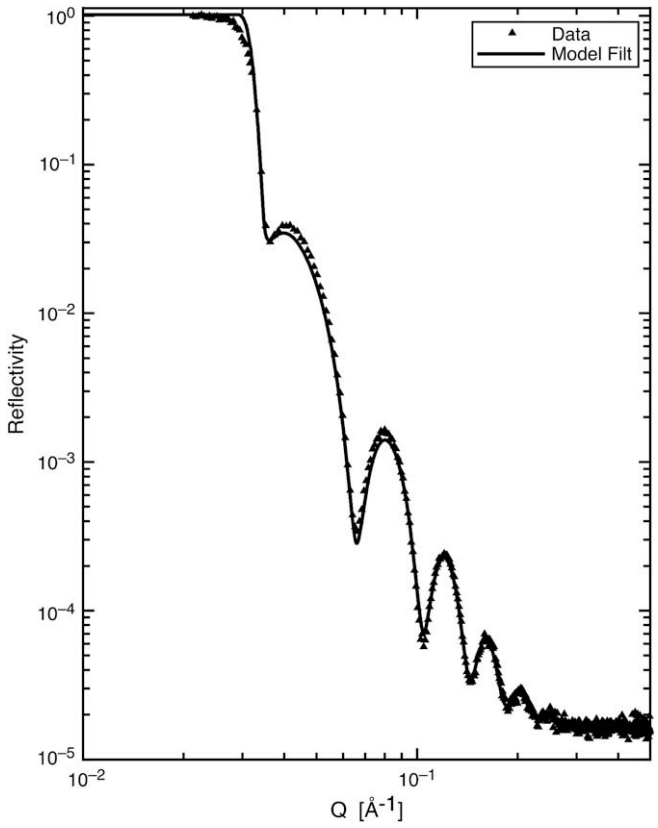

Fig. 6. X-ray reflectivity data for a typical dry brush layer synthesized using the protected monomer route, having a dry thickness of 156 Å and a surface roughness of 5 Å.

3.2. Molecular weight determination of a grafted poly(methacrylic acid) brush using single molecule force spectroscopy

Direct determination of the molecular weight of a grafted polymer brush is very difficult to obtain using standard analytical methods, owing to the small amount of brush material and the difficulties involved in removing the grafted layer from the substrate without destroying it. Standard practice is to use untethered free initiator and then carry out GPC on this material and assume that the free initiator and surface bound initiator produce the same molecular weight polymer. Using this method, we found that the brush was of poor quality as it was coated with a layer of untethered polymer. Instead we decided to measure the M_W directly using force pulling methods, which have been used extensively to evaluate the molecular weight of grafted polymer brushes [39–42].

The force pulling profile for a grafted polymer brush has a maximum attractive force, which decays towards zero upon increasing chain extension. The total number of stretched chains decreases with increasing extension, as progressively longer chains approach their contour lengths and break free from the tip. The preferred way to determine the molecular weight was to measure it directly by measuring single molecule force–distance curves and determining the contour length ($L_{contour}$) for single molecule stretching events, where the maximum $L_{contour}$ would be related to the upper limit of the molecular weight of the polymer brush. The worm like chain model (WLC) model was used to fit the single molecule force extension curves for the brush force pulling experiments. In the WLC model F_{chain} is the elastic restoring force of the polymer chain, x is the chain end-to-end separation distance and k_B is the Boltzmann constant. The persistence length is l_p, T is the absolute temperature and $L_{contour}$ is the fully extended contour length of the chain.

$$F_{chain} = \left(\frac{k_B T}{l_p}\right)\left(\frac{1}{4}\left(1-\frac{x}{L_{contour}}\right)^{-2}-\frac{1}{4}+\frac{x}{L_{contour}}\right)$$

The persistence length l_p of poly(methacrylic acid) is a fixed parameter in the WLC model using the value from the literature of 5 Å determined using small angle X-ray scattering for ungrafted PMAA [43]. The value of the persistence length should be valid as it a basic property of PMAA whether or not it is grafted to a surface. Constraining the persistence length requires that only one parameter is fitted to the WLC model and removes some ambiguity in the data analysis. This persistence length value proves to be very accurate for all of the data used to evaluate the molecular weight of the brush. The suitability of fixing this parameter can be seen in Fig. 7, where deviation from the fixed value of 5 Å is only seen at large extensions. This is the case for most polymers fitted to worm like chain or freely jointed chain models as they break down at high extensions. Single molecule stretching events were collected in deionized water for multiple sites on the brush to get a meaningful data set. To best evaluate the molecular weight of the brush only the final pull event for each approach-retract curve was fitted as this gives the best estimate of the contour length immediately prior to the tip pulling away from the brush. All of the terminal force pulling events were fitted to the WLC model using a fixed persistence length to give a distribution of contour lengths $L_{contour}$. The fitted contour length is an integer N times the persistence length l_p.

From the distribution of measured terminal contour lengths, a molecular weight, M_i can be determined from:

$$M_i = \frac{M_0 L_c}{l_p} \quad (1)$$

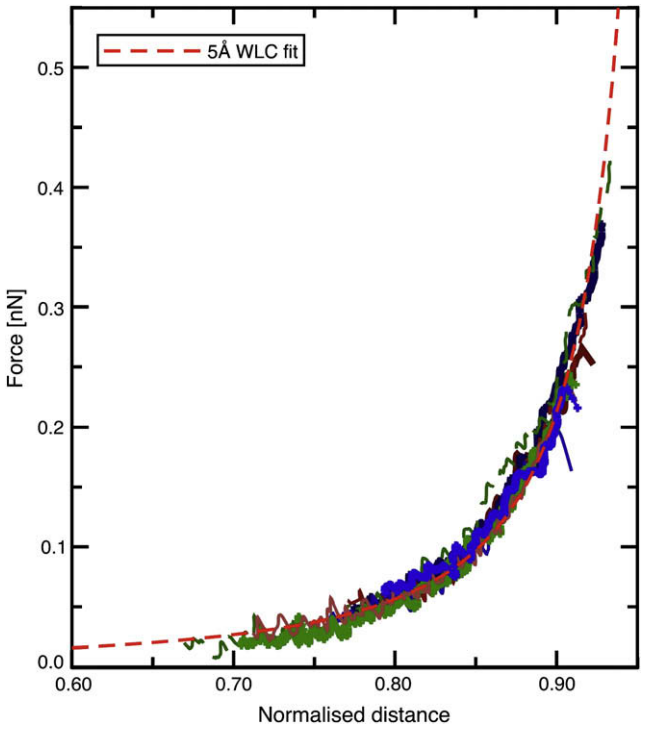

Fig. 7. Single molecule stretching events fitted using the worm like chain model with a fixed persistence length of 5 Å and normalized by their contour length, $L_{contour}$.

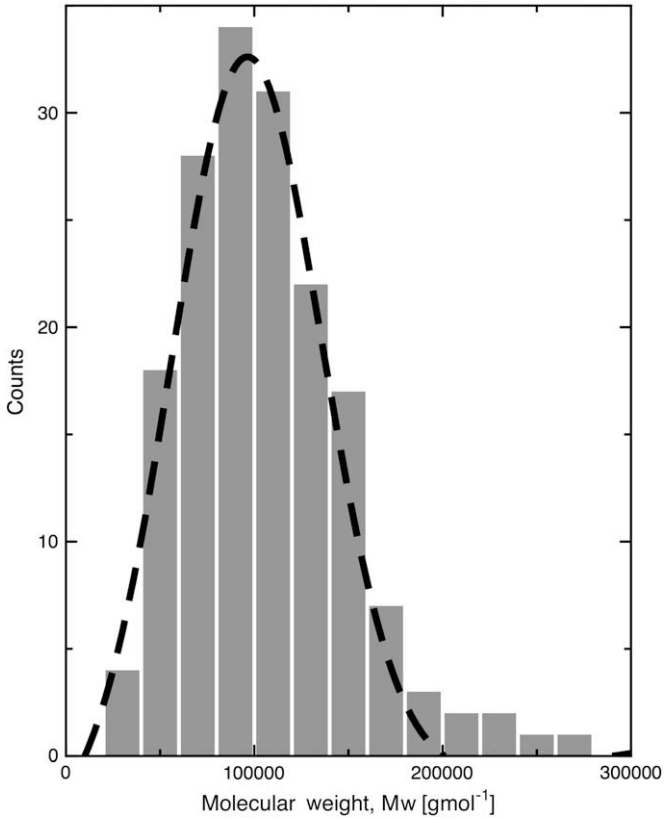

Fig. 8. The distribution of measured molecular weights evaluated from the worm like chain fitted contour lengths, $L_{contour}$ of a PMAA polymer brush.

where M_0 is the individual monomer molecular weight, which is 86 g mol^{-1} for a methacrylic acid monomer unit (Fig. 8).

The molecular weight data from the force pulling gives an average M_n of 106,000 g mol^{-1}, M_w of 124,000 g mol^{-1} and polydispersity of 1.15. The force pulling data probably give an overestimate of molecular weight, due to the increased likelihood that longer chains will be subjected to pulling events, and this is also expected to affect the measured polydispersity. Countering this however is the fact that the AFM tip is highly unlikely to interact with the very end of the PMAA chain. However this is expected to be a small effect because chain ends are expected to be near the surface for an ATRP polymerization. Despite these complications, we conclude that force pulling measurements are an effective way of measuring the brush molecular weight.

3.3. Grafting density

The grafting density of the polymer brushes was calculated using the molecular weight extracted from the HRFS data. The data in Fig. 9 show the effect of the grafting density on brush height. For such samples the silicon surface can be controlled to give different grafting densities by using a "dummy" initiator. This was done using a trichlorosilane with an almost identical length to the initiator, but incapable of initiating brush growth. This has the effect of reducing the number of possible initiating sites on the surface and means that the chains are much further separated than if the surface were coated with 100% initiator sites, lowering the grafting density. The assumption was then made for the dummy initiator that the proportions allowed a reduction in the grafting density according to the proportions of the mixture of dummy initiator and standard initiator. We assume that the brush growth kinetics are not altered by the use of dummy initiator.

The grafting density Γ of a polymer brush was calculated for the dry polymer brush layer using Eq. (2).

$$\Gamma = \left(\frac{h\rho N_A}{M_N}\right) \tag{2}$$

where h is the brush height, ρ is the density of the polymer, N_A is Avagadro's constant and M_N is the number averaged molecular weight. The density of PMAA is assumed to be the same as its bulk density of 1.015 g cm^{-3} [44]. For a brush with full surface initiator coverage and an M_N value of 106,000 gmol^{-1} from the HRFS data, the surface grafting density was calculated to be 0.12 chains nm^{-2}. The distance between the grafting sites d was calculated to be 3.2 nm using:

$$d = \left(\frac{4}{\Gamma\pi}\right)^{\frac{1}{2}} \tag{3}$$

The force pulling data gave a derived grafting density for the 100% initiator case that then allowed the calculation of the grafting density with the non-initiating silane.

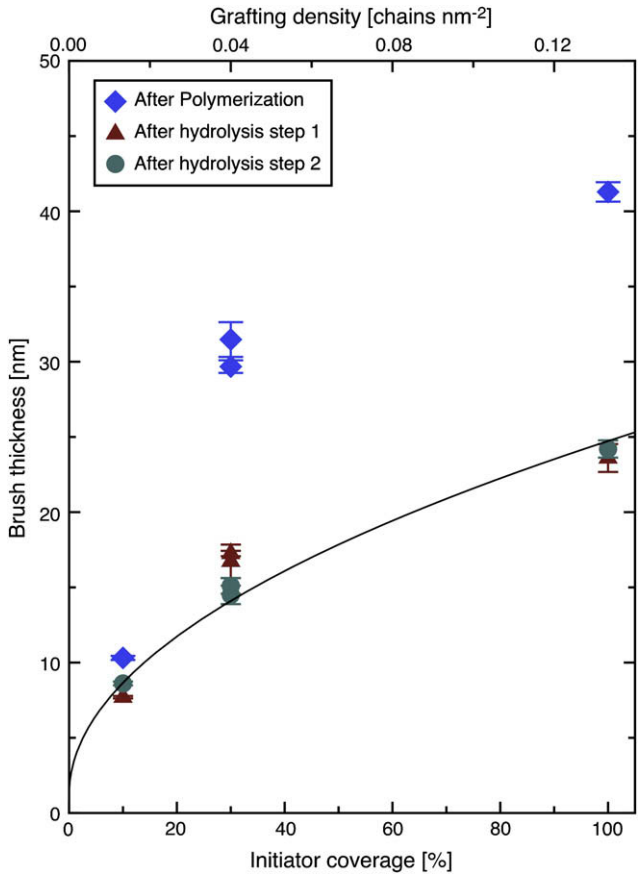

Fig. 9. Thickness measurements measured using ellipsometry for a series of brushes synthesized using the protected monomer route with three different surface initiator densities made of mixed monolayer of ATRP initiating and non-initiating species.

3.4. pH dependent swelling

There have so far been few experiments to probe the height change in a polyelectrolyte brush in response to changes in the environmental pH and salt concentration. One study used neutron reflectometry to examine the pH response of a weak polybase of poly[2-(diethyl amino)ethyl methacrylate] and observed a shift in the pK_a as a function of the grafting density [38]. The pH at which the brush starts to swell is a critical aspect in the behaviour of polyelectrolyte brushes.

The data displayed in Fig. 10 show that the brush layer begins to swell at pH 7 and continues swelling up until pH 10.5 whereupon the layer starts to collapse, possibly due to the presence of an excess of salt ions in the system [45]. With increasing pH, poly(methacrylic acid) chains in solution transform from a collapsed to stretched conformation around pH = pK_a. This conformational change is induced by the electrostatic repulsion between the carboxylate anions. The equilibrium chain conformation is a balance between the electrostatic interaction of the charged carboxylate anion groups, which favours stretching, and the conformational entropy of the PMAA chains, which opposes stretching. The AFM images for the two extremes of the brush state are shown to highlight the effect of the pH change and to show that the same area of brush has been used to quantify the swelling of the polyelectrolyte brush layer. Fluorescence measurements for dilute untethered PMAA reveal that the transition for this system is much lower in pH, with a conformational shape transition at pH 5.5 [46]. There is therefore a massive difference between the two regimes of tethered and untethered, that exists entirely due to the highly grafted nature of the polymer chains to a substrate [5,47]. Currie et al. have also observed a shift in the observed swelling of grafted poly(acrylic acid) brush layers and attribute it to a displacement of the effective pK_a of the brush as the overall degree of dissociation α decreases strongly with increasing grafting density. The explanation for the shift in the effective pK_a of the brush is ultimately a result of the high degree of Coulombic repulsion of neighbouring charges. The distance between the carboxylate anions is controlled by the Bjerrum length of the mixture. Forcing the polyacid chains together

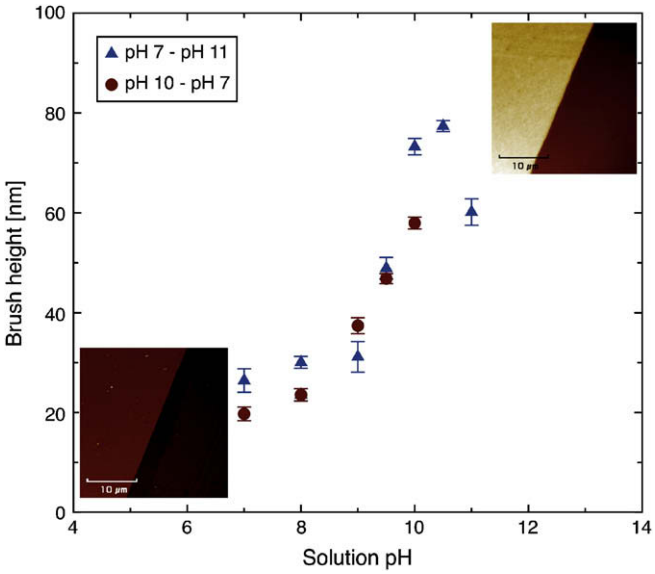

Fig. 10. AFM brush height measurements for the swelling and de-swelling cycle for a poly(methacrylic acid) brush as the pH of the solution is altered from pH 7 to pH 11 and reversed from pH 10 back to pH 7. The brush has a dry thickness of 21 nm as measured by ellipsometry, an average M_W of 124,000 gmol^{-1} and a grafting density of 0.12 chains nm^{-2}.

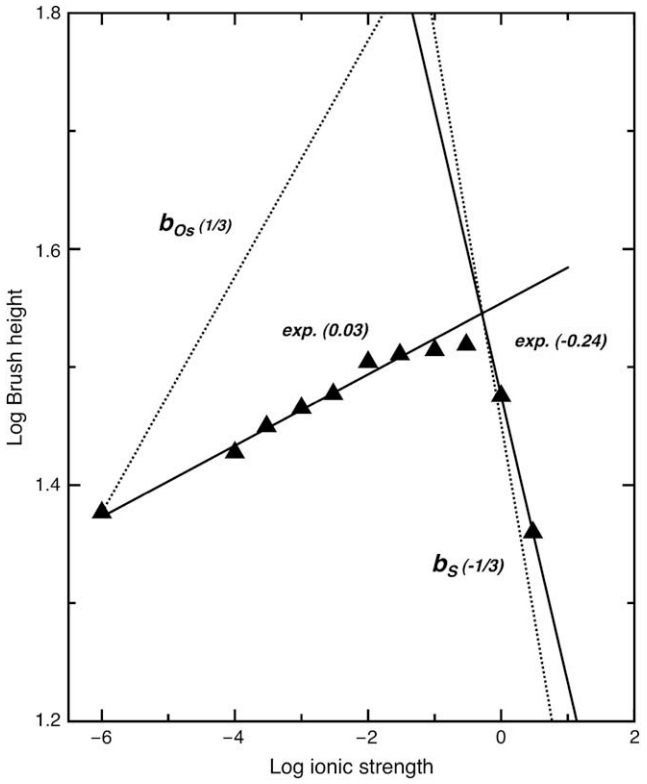

Fig. 11. Thickness change for a poly(methacrylic acid) brush as a function of the sodium ion concentration at a fixed pH of 6. The predicted theoretical scaling relationships for the osmotic brush state (b_{Os}) and the salted brush state (b_s) are plotted as dotted lines with the exponents in italics. The observed exponents from the experiment are plotted with solid lines and points with the values for the measured exponents in italics.

therefore causes counterion condensation, which avoids frustration of excess charge in such a confined system. Dissociation of the weak acid groups within the brush layer will therefore only be complete at higher pH values in solution relative to that of a weak acid in the bulk phase. This increase of the pK_a to 9 is a good deal more than that seen for an ungrafted carboxylic acid group which has a pK_a of 4 [48].

3.5. Monovalent salt ions

A systematic study was carried out to examine the influence of added monovalent sodium (Na^+) salt ions. The brush was investigated at a fixed pH of 5.9 using milli Q pure deionized water. The same area of sample was measured throughout the experiment to give a consistent method for measuring the effect of the ionic strength on the brush height.

The brush swells from an initial thickness of 24 nm at a salt concentration of 1 μM to a maximum thickness of 33 nm at 0.3 M and then collapses as the salt concentration is increased beyond 0.3 M.

The data in Fig. 11 are presented in a double logarithmic plot of the brush thickness as a function of ionic strength because this gives a way to compare the data to the theoretical mean field power law proposed by Zhulina et al. [14]. Here it is proposed, that in the osmotic brush regime, the brush height scales as a function of ionic strength, $h \propto I^{1/3}$ for a given pH and a fixed grafting density. There is qualitative agreement between our data and the mean field predictions for an osmotic brush in that it shows two distinct regimes. The results clearly show that the exponent for this brush system is significantly smaller with a brush height increase for the osmotic brush regime of $\sim I^{1/30}$. This large difference between the experimental data and theory may be due to the analytical model neglecting important steric contributions, which are expected to play an important role for closely packed polymer chains. Table 2 is a summary of experiments where we can compare the exponents for the osmotic brush and the salted brush for comparable weak polyelectrolyte systems. The only set of data that shows an agreement with the theoretical model of Zhulina et al. for the osmotic brush state is the study carried out by Biesalski et al., whose study concerns non-densely grafted chains with a polydispersity of 2. The other studies all show a much weaker dependence with exponents ranging from 0.0 to 0.11. The agreement between the salted brush regime experiments seems to be more consistent values closer to the predicted exponent of 0.33, although we have limited data to draw a full conclusion for the salted regime.

The transition from the osmotic brush to the salted brush regime occurs when the bulk salt concentration is equal to the free mobile counterion concentration [49]. This point happens at a sodium ion concentration of 0.3 M, which corresponds to a Debye length of 6 Å. A simple calculation using the areal density, thickness and molecular weight allow us to estimate the degree of ionization in the brush, which gives $\alpha \approx 0.05$, where $\alpha = 1$ means that the

Table 2
Summary of the measured exponents for the osmotic brush state (b_{Os}) and the salted brush state (b_s) for poly(acrylic acid) or PAA and poly(methacrylic acid) or PMAA end-anchored or chemically end-grafted weak polyelectrolyte brush layers. Γ is the grafting density of the brushes in units of chains nm^{-2}.

Polymer	Γ [chains nm^{-2}]	b_{Os}	b_S	Technique	Reference
PAA	0.125–0.39	0.1	–	Ellipsometry	Currie et al. [5]
PAA	0.039	0.03	−0.3	DLS	Guo et al. [50]
PAA	0.718	0	−0.31	SAXS	Bendejacq et al. [51]
PAA	0.143	0.03	–	Ellipsometry	Wu et al. [52]
PMAA	0.005–0.116	0.11	−0.10	Ellipsometry	Zhang et al. [47]
PMAA	0.025	0.33	−0.33	Ellipsometry	Biesalski et al. [17]
PMAA	0.123	0.03	−0.24	AFM	This study

brush is fully dissociated. Further work will examine the effect of adding salt at higher values of pH.

4. Conclusions

We have successfully prepared stimuli-responsive poly(methacrylic acid) brushes on planar silicon surfaces using atom transfer radical polymerization of EEMA, which was converted to PMAA by hydrolysis. The grafted polymer brushes were characterized by determining the molecular weight via single molecule force spectroscopy, which then enabled the determination of the grafting density. The deprotection of the EEMA precursor was assessed by transmission FT-IR with the presence of a broad peak at 3200 cm^{-1} which indicates an OH group. The swelling properties of the brushes in aqueous liquids confirm a rich responsive polyelectrolytic behaviour. AFM measurements show pH dependent swelling to take place well above pH 7 with a maximum swelling at pH 10.5, well above the pK_a of free poly(methacrylic acid). The salt swelling of the brush shows a transition from the osmotic brush to the salted brush as the concentration of monovalent salt ions was increased.

Acknowledgement

Funding for this work came from the EPSRC for AJP, GR/T11562 and SM, GR/NO2542. We thank Jamie Hobbs and Cvetelin Vasilev for their assistance and advice with the AFM measurements and Irfan Arif for carrying out the XPS measurements.

Appendix. Supporting information

Supplementary data associated with this article can be found in the online version at doi:10.1016/j.polymer.2008.11.051.

References

[1] Joerg L, Mitragotri S, Tran T, Kaido H, Sundaram J, Choi IS, et al. Science 2003;299:371.
[2] La Spina R, Tomlinson MR, Ruiz-Pérez L, Chiche A, Langridge S, Geoghegan M. Angew Chem Int Ed 2007;46:6460–3.
[3] Zhou F, Shu W, Welland ME, Huck WTS. J Am Chem Soc 2006;128:5326–7.
[4] Parnell AJ, Martin SJ, Jones RAL, Vasilev C, Crook CJ, Ryan AJ. Soft Matter, in press, doi:10.1039/b812872c.
[5] Currie EPK, Sieval AB, Fleer GJ, Stuart Cohen. Langmuir 2000;16(22):8324–33.
[6] Advincula RC, Brittain WJ, Caster KC, Rühe J, editors. Polymer brushes: synthesis, characterization, applications. Wiley; 2004.
[7] Zhao B, Brittain WJ. Prog Polym Sci 2000;25:677–710.
[8] Bumbu GG, Kircher G, Wolkenhauer M, Berger RGJS. Macromol Chem Phys 2004;205(12):1713–20.
[9] Alexander S. J Phys (Paris) 1977;38(8):983.
[10] Jones RAL, Richards RW. Polymers at surfaces and interfaces. Cambridge: Cambridge University Press; 1999.
[11] Tokarev I, Minko S. Soft Matter, in press, doi:10.1039/b813827c.
[12] Boyes SG, Granville AM, Baum M, Akgun B, Mirous BK, Brittain WJ. Surf Sci 2004;570(1):1–12.
[13] Zhulina EB, Wolterink JK, Borisov OV. Macromolecules 2000;33:4945–53.
[14] Zhulina EB, Birshtein TM. Macromolecules 1995;28:1491–9.
[15] Lyatskaya YV, Leermakers FKM, Fleer GJ, Zhulina EB, Birshtein TM. Macromolecules 1995;28(10):3562–9.
[16] Israëls R, Leermakers FAM, Fleer GJ. Macromolecules 1994;27(11):3087–93.
[17] Biesalski M, Johannsmann D, Rühe J. J Chem Phys 2002;117:4988–94.
[18] Rühe J, Ballauff M, Biesalski M, Dziezok P, Göhn F, Johannsmann D, et al. Adv Polym Sci 2004;165:79–150.
[19] Matyjaszewski K, Xia JH. Chem Rev 2001;101:2921–90.
[20] Farhan T, Azzaroni O, Huck WTS. Soft Matter 2005;1:66.
[21] Kaholek M, Lee WK, Ahn SJ, Ma H, Caster KC, LaMattina B, et al. Chem Mater 2004;16:3688.
[22] Ryan AJ, Crook CJ, Howse JR, Topham P, Geoghegan M, Martin SJ, et al. J Macromol Sci B 2005;44:1103–21.
[23] Iscoff R. Semicond Int 1993;16:58–63.
[24] Beers KL, Gaynor SG, Matyjaszewski K, Sheiko SS, Möller M. Macromolecules 1999;31:9413–5.
[25] Nakagawa Y, Miller PJ, Matyjaszewski K. Polymer 1998;39(21):5163–70.
[26] Topham PD, Howse JR, Crook CJ, Parnell AJ, Geoghegan M, Jones RAL, et al. Polym Int 2006;55:808–15.
[27] Zhang H, Ruckenstein E. Macromolecules 1998;31:7575–80.
[28] Camp WV, Prez FED. Macromolecules 2004;37(18):6673–5.
[29] Ryan AJ, Crook CJ, Howse JR, Topham P, Jones RAL, Geoghegan M, et al. Faraday Discuss 2005;128:55–74.
[30] Treat ND, Ayres N, Boyes SG, Brittain WJ. Macromolecules 2006;39:26–9.
[31] Hutter JL, Bechoefer J. Rev Sci Instrum 1993;64:1868.
[32] Seog J, Dean D, Plaas AHK, Wong-Palms S, Grodzinsky AJ, Ortiz C. Macromolecules 2002;35:5601–15.
[33] Jones RAL, Norton LJ, Shull KR, Kramer EJ, Felcher GP, Karim A, et al. Macromolecules 1992;25:2359.
[34] Leckner J. Theory of reflection. Dordrecht: Martinus Nijhoff; 1987.
[35] Névot L, Croce P. Rev Phys Appl (Paris) 1980;15:761.
[36] Shen Y, Zhu S. Macromolecules 2001;34:8603.
[37] Chyan OMR, Wu J, Chen J-J. Appl Spectrosc 1997;51:1905–9.
[38] Geoghegan M, Ruiz-Pérez L, Dang CC, Parnell AJ, Martin SJ, Howse JR, et al. Soft Matter 2006;2(12):1076.
[39] Goodman D, Kizhakkedathu JN, Brooks DE. Langmuir 2004;20(15):6238–45.
[40] Goodman D, Kizhakkedathu JN, Brooks DE. Langmuir 2004;20(6):2333–40.
[41] Goodman D, Kizhakkedathu JN, Brooks DE. Langmuir 2004;20(8):3297–303.
[42] Al-Maawali S, Bemis JE, Akhremitchev BB, Leecharoen R, Janesko BG, Walker GC. J Phys Chem B 2001;105(18):3965–71.
[43] Muroga Y, Yoshida T, Kawaguchi S. Biophys Chem 1999;81(1):45–57.
[44] Bell CL, Peppas NA. Biomaterials 1996;17:1203–18.
[45] Crook CJ, Smith A, Jones RAL, Ryan AJ. Phys Chem Chem Phys 2002;4:1367–9.
[46] Ruiz-Pérez L, Pryke A, Sommer M, Battaglia G, Soutar I, Swanson L, et al. Macromolecules 2008;41:2203.
[47] Zhang H, Rühe J. Macromolecules 2005;38:4855–60.
[48] Wang J, Frostman LM, Ward MD. J Phys Chem 1992;96:5224.
[49] Balastre M, Li F, Schorr P, Yang JC, Mays JW, Tirrell MV. Macromolecules 2002;35:9480.
[50] Guo X, Ballauf M. Phys Rev E 2001;64(051406).
[51] Bendejacq D, Ponsinet V, Joanicot M. Eur Phys J E 2004;13:3–13.
[52] Wu T, Gong P, Szleifer I, Vlček P, Šubr V, Genzer J. Macromolecules 2007; 40(24):8756–64.